Stem Cell Research 44 (2020) 101749

Contents lists available at ScienceDirect

Stem Cell Research

journal homepage: www.elsevier.com/locate/scr

Modeling of early neural development *in vitro* by direct neurosphere formation culture of chimpanzee induced pluripotent stem cells

Ryunosuke Kitajima[a,1], Risako Nakai[a,1], Takuya Imamura[b], Tomonori Kameda[b], Daiki Kozuka[a], Hirohisa Hirai[a], Haruka Ito[a], Hiroo Imai[a], Masanori Imamura[a,1,*]

[a] Molecular Biology Section, Department of Cellular and Molecular Biology, Primate Research Institute, Kyoto University, Inuyama, Aichi 484-8506, Japan
[b] Department of Stem Cell Biology and Medicine, Graduate School of Medical Sciences, Kyushu University, Maidashi 3-1-1, Higashi-ku, Fukuoka 812-8582, Japan

ARTICLE INFO

Keywords:
Chimpanzee
iPSCs
In vitro differentiation
Neural development

ABSTRACT

Evolutionary developmental biology of our closest living relative, the chimpanzee (*Pan troglodytes*), is essential for understanding the origin of human traits. However, it is difficult to access developmental events in the chimpanzee *in vivo* because of technical and ethical restrictions. Induced pluripotent stem cells (iPSCs) offer an alternative *in vitro* model system to investigate developmental events by overcoming the limitations of *in vivo* study. Here, we generated chimpanzee iPSCs from adult skin fibroblasts and reconstructed early neural development using *in vitro* differentiation culture conditions. Chimpanzee iPSCs were established using straightforward methods, namely, lipofection of plasmid vectors carrying human reprogramming factors, combined with maintenance in a comprehensive feeder-free culture. Ultimately, direct neurosphere formation culture induced rapid and efficient differentiation of neural stem cells from chimpanzee iPSCs. Time course analysis of neurosphere formation demonstrated ontogenetic changes in gene expression profiles and developmental potency along an early neural development path from epiblasts to radial glia. Our iPSC culture system is a potent tool for investigating the molecular and cellular foundation underlying chimpanzee early neural development and better understanding of human brain evolution.

1. Introduction

The molecular foundation of neural development in primates is of importance to evolutionary developmental (Evo-Devo) biology of human brain evolution. Early neural development in mammals is a highly coordinated sequential event under spatiotemporal control, which originates from epiblast differentiation. The pluripotent epiblast is the origin of all somatic lineages in the three primary germ layers (ectoderm, mesoderm, and endoderm). The anterior neuroectoderm is the first derivative committed to a neural fate, and is induced from the late epiblast by exposure of mesodermal organizer-derived native inhibitors against bone morphogenic protein (BMP) and activin/nodal signaling (Ozair et al., 2013). Neuroepithelial cells form a single layered neural plate. They begin infolding from the neural grove to construct the neural tube while dividing symmetrically to increase their number. Subsequently, the anterior portion of the neural tube expands to organize neuromeres, which are transient structures of the early developing brain. At this stage, neuroepithelial cells transform into radial glia with long processes called radial fibers in the ventricular zone of the forebrain, and acquire neurogenic potency in response to Notch signaling (Merkle and Alvarez-Buylla, 2006; Kageyama et al., 2008). Neuroepithelial cells and radial glia possess neural stem cell (NSC) properties during early neural development, therefore their developmental potency can be regarded as an important determinant of brain size evolution (Kriegstein et al., 2006; Borrell and Reillo, 2012).

To understand the Evo-Devo aspect of human brain evolution, it is essential to clarify the molecular and cellular differences between humans and chimpanzees (as our closest living relatives), and when these differences emerge during neural development (Cheng et al., 2005; Kronenberg et al., 2018). However, unlike mice and rats, technical and ethical restrictions make it difficult to address Evo-Devo studies of humans and chimpanzees. These restrictions include limited availability of tissue materials, inaccessibility to embryos, and issues against invasive approaches and genetic manipulations. To compensate for these *in vivo* issues, induced pluripotent stem cells (iPSCs) (Takahashi et al., 2007) can serve as an alternative *in vitro* strategy for human Evo-Devo studies. First, iPSCs can be generated from small biopsy samples of various tissues with relatively easy methods. Second,

* Corresponding author.
E-mail address: imamura.masanori.2m@kyoto-u.ac.jp (M. Imamura).
[1] Contributed equally.

https://doi.org/10.1016/j.scr.2020.101749
Received 24 September 2019; Received in revised form 17 January 2020; Accepted 21 February 2020
Available online 28 February 2020

iPSCs self-renew robustly and infinitely, which enables a sufficient amount of cell material to be obtained for experiments. Third, iPSCs can differentiate into all three germ layers and germ cells, therefore it is possible to reconstruct developmental events by *in vitro* differentiation culture. Fourth, iPSCs are amenable to genetic manipulations such as genome editing. Altogether, iPSCs provide a potent *in vitro* model system for the non-invasive dissection of developmental events of interest in humans and chimpanzees (Prescott et al., 2015; Otani et al., 2016; Mora-Bermudez et al., 2016; Field et al., 2019; Marchetto et al., 2019; Pollen et al., 2019).

To monitor early neural development in chimpanzee *in vitro*, in this study, we generated chimpanzee iPSCs from adult skin fibroblasts by lipofection of plasmid vectors carrying human reprogramming factors, and cultured these iPSCs using comprehensive feeder-free cultures. These chimpanzee iPSCs reconstruct early neural development by direct neurosphere formation culture (Nakai et al., 2018) with dorsomorphin and SB431542, small molecule inhibitors of BMP and activin/nodal signaling (Morizane et al., 2011). During neurosphere formation, stepwise changes in gene expression profiles and developmental potency were observed in accordance with ontogenetic early neural development. Thus, our *in vitro* differentiation system of chimpanzee iPSCs is a convenient tool for human Evo-Devo studies to address the molecular pathways underlying early neural development.

2. Material and methods

2.1. Ethics

All experiments using primate samples were approved by the Animal Care and Use Committee of Kyoto University Primate Research Institute (KUPRI) and were performed in accordance with the Guidelines for Care and Use of Nonhuman Primates (Version 3, 2010) published by KUPRI.

2.2. Primary culture of chimpanzee fibroblasts

Chimpanzee fibroblasts were isolated from skin specimens of three individuals: Kenny (GAIN-ID: 0363, 24-year-old male), Mari (GAIN-ID: 0274, 39-year-old female), and Kiku (GAIN-ID: 0138, 39-year-old female). To establish primary fibroblast cultures, skin specimens were minced into 2–3 mm pieces with scissors, placed on 0.1% gelatin-coated culture plates, and incubated in 15% fetal bovine serum (FBS)/Dulbecco's modified Eagle's medium (DMEM) with high glucose (044-29765; Wako, Osaka, Japan) supplemented with 15% FBS, 1 × non-essential amino acids (139-15651; Wako), 2 mM L-glutamine (073-05391; Wako), 1 mM sodium pyruvate (190-14881; Wako), 0.11 mM 2-mercaptoethanol (21985-023; Gibco, Waltham, MA, USA), and 100 U/ml penicillin and 100 μg/ml streptomycin (168-23191; Wako) at 37 °C with 5% CO_2. Migration of fibroblasts was observed after 1-week of culture. The cells were then transferred to new culture plates by trypsinization with 0.25% trypsin/ethylenediaminetetraacetic acid (EDTA).

2.3. Generation of chimpanzee iPSCs with episomal plasmids under feeder-free conditions

The day before gene transduction, primary fibroblasts were plated at 1.5×10^5 cells/well in Geltrex (A1569601; Gibco)-coated 6-well culture plates with 15% FBS/DMEM. Cells were transfected with 2 μg of pCXLE-EGFP (27082; Addgene, Watertown, MA, USA) or combined pCXLE-hOCT3/4-shp53-F (27077; Addgene), pCXLE-hUL (27080; Addgene), and pCXLE-hSK (27078; Addgene) using ViaFect transfection reagent (E4981; Promega, Madison, WI, USA), according to the manufacturer's instructions. Transfected cells were cultured in Essential 6 (A1516401; Gibco) supplemented with 100 ng/ml basic fibroblast growth factor 2 (FGF2) (100-18B; PeproTech, Rocky Hill, NJ, USA) and 100 nM hydrocortisone (088-02483; Wako) for 4 days. Then, the medium was exchanged to Essential 6 supplemented with 10 ng/ml FGF2 and 100 μM sodium butyrate (303410–5G; Sigma-Aldrich, St. Louis, MO, USA) every 3 days. Subsequently, iPSC colonies appeared on days 20–30 after transfection. Individual colonies were picked into iMatrix-511 (389-07364 or 383-10133; Matrixome, Osaka, Japan)-coated culture plates and expanded with StemFit medium (AK02N; Ajinomoto, Tokyo, Japan).

2.4. Maintenance culture of chimpanzee iPSCs

Chimpanzee iPSCs were maintained in StemFit medium on iMatrix-511-coated culture plates. The medium was usually exchanged on days 1, 3, 5, and 6 after every passage. On day 7, cells were dissociated to single cells with TrypLE Express (12604021; Gibco), and then replated at 3×10^4 cells/dish into iMatrix-511-coated 60-mm culture dishes with StemFit medium and 10 μM Y-27632 (253-00513; Wako).

2.5. Chromosome analysis

Chimpanzee iPSCs at 70–80% confluency were treated with 20 ng/ml KaryoMAX Colcemid Solution (15212012; Gibco) for 3 h. Cells were harvested by incubation with TrypLE Express, treated with 0.56% KCl for 20 min at room temperature, and then fixed with ethanol–acetic acid (3:1) for 10 min on ice. Chromosome spreads were prepared using one drop of fixed cell suspension. Chromosome preparations were dried in a 37 °C incubator for 1-week and then stored at −80 °C until staining. Chromosome samples were treated with 0.005% trypsin/EDTA for 30 s, neutralized with 0.05% FBS, and stained with Giemsa solution for 5 min. Karyotyping was performed in accordance with a chromosome ideogram (Yunis et al., 1980).

2.6. Alkaline phosphatase and rBC2LCN-FITC staining

Alkaline phosphatase staining was performed using the Leukocyte Alkaline Phosphatase kit (86R-1KT; Sigma-Aldrich), according to the manufacturer's instructions. For rBC2LCN-FITC staining, cells were fixed with 4% paraformaldehyde for 15 min at room temperature. After washing with phosphate-buffered saline, cells were treated with rBC2LCN-FITC (1:100) (180-02991; Wako) for 1 h at room temperature.

2.7. Immunofluorescence analysis

Cells were fixed with 4% paraformaldehyde, permeabilized with 0.5% Triton X-100, blocked with 5% skimmed milk or 20% ImmunoBlock (CTKN001; KAC, Kyoto, Japan), and incubated with primary antibodies. The following primary antibodies were used: mouse anti-OCT4 (611202; BD Biosciences, San Jose, CA, USA), mouse anti-SOX2 (MAB2018; R&D Systems, Minneapolis, MN, USA), rabbit anti-NANOG (ab109250; Abcam, Cambridge, UK), rabbit anti-SALL4 (ab29112; Abcam), goat anti-LIN28A (AF3757; R&D Systems), rabbit anti-DPPA4 (ab24308; Abcam), mouse anti-TRA-1-81 (MAB4381; Millipore, Burlington, MA, USA), rat anti-SSEA3 (MAB4303; Millipore), mouse anti-SSEA4 (MAB4304; Millipore), mouse anti-E-cadherin (610182; BD Biosciences), mouse anti-keratan sulfate (R-10G) (011–25811; Wako), mouse anti-tubulin β3 (801201; BioLegend, San Diego, CA, USA), mouse anti-nestin (MAB5326; Millipore), mouse anti-α-smooth muscle actin (SMA) (ab7817; Abcam), rabbit anti-vimentin (ab92547; Abcam), goat anti-SOX17 (AF1924; R&D Systems), mouse anti-alpha-fetoprotein (AFP) (MAB1369; R&D Systems), rabbit anti-PAX6 (901301; BioLegend,), goat anti-OTX2 (AF1979; R&D Systems), rabbit anti-FOXG1 (ab18259; Abcam), rabbit anti-BRN2 (GTX114650; GeneTex, Irvine, CA, USA), rabbit anti-microtubule-associated protein 2 (MAP2) (AB5622; Millipore), mouse anti-drebrin (015-27271; Wako), and rabbit anti-S100β (ab52642; Abcam). The secondary antibodies were: Alexa Fluor 488 goat anti-mouse IgG (A11011 or A32723;

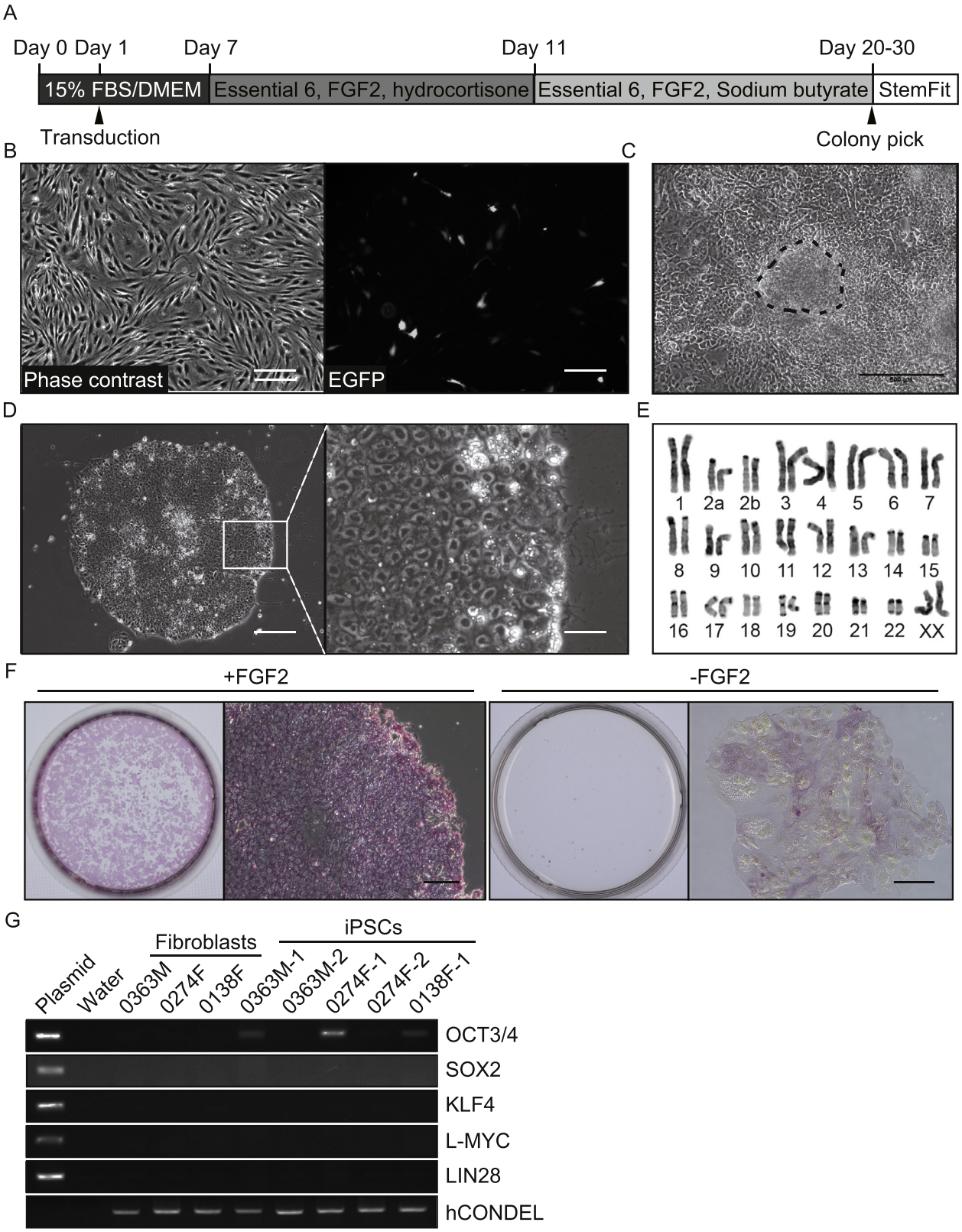

Fig. 1. Generation of chimpanzee iPSCs.
A. Schematic design of chimpanzee iPSC generation. B. Expression of EGFP transgene in fibroblasts 24 h after transduction. Scale bar: 500 μm. C. Phase contrast image of an emerging chimpanzee iPSC colony. The iPSC colony shown by a dotted circle was picked. Scale bar: 500 μm. D. Phase contrast image of chimpanzee iPSCs (0138F-1) at passage 8. Scale bars: 200 μm (left) and 50 μm (right). E. Chromosome analysis of chimpanzee iPSCs (0138F-1, passage 22). F. Alkaline phosphatase staining of chimpanzee iPSCs (0138F-1) cultured in the presence or absence of fibroblast growth factor 2. Scale bar: 100 μm. G. Genomic PCR of transgenes. Genomic DNA was isolated from five chimpanzee iPSC lines (0363M-1, 0363M-2, 0274F-1, 0274F-2, and 0138F-1) and three parental fibroblast lines (0363 M, 0274F, and 0138F). A hCONDEL region was used as an internal control. Each plasmid vector carrying reprogramming factors and water were used as positive and negative controls, respectively.

Thermo Fisher Scientific, Waltham, MA, USA), Alexa Fluor 488 donkey anti-goat IgG (A11055; Thermo Fisher Scientific), Alexa Fluor 555 donkey anti-mouse IgG (ab150110; Abcam), Alexa Fluor 555 donkey anti-rabbit IgG (A31572; Thermo Fisher Scientific), and Alexa Fluor 488 goat anti-rat IgG (ab150157, Abcam). Nuclei were stained with 1 μg/ml 4′,6-diamidino-2-phenylindole (DAPI) (D523; Dojindo, Kumamoto, Japan). For each experiment, a negative control was included in which the primary antibody had been omitted. Images were captured using a BZ-X700 fluorescence microscope (Keyence, Osaka, Japan).

2.8. RT-PCR, genomic PCR, and quantitative PCR analyses

Total RNA was extracted using RNeasy Plus Mini Kit (74104; Qiagen, Hilden, Germany) and reverse transcribed using PrimeScript RT reagent kit with gDNA Eraser (RR047A; Takara, Shiga, Japan). Genomic DNA was isolated using DNeasy Blood & Tissue Kit (69506; Qiagen). RT-PCR and genomic PCR analyses were performed with ExTaq Hot Start Version (RR006A; Takara). All experiments were performed semi-quantitatively at three different amplification cycles. Representative images are shown. For quantitative PCR, THUNDERBIRD SYBR qPCR Mix (QPS-201; Toyobo, Osaka, Japan) and StepOne (Applied Biosystems, Foster City, CA, USA) were used.

2.9. Transcriptome analyses

For directional RNA-Seq library construction, three replicates were made using the NEBNext Ultra Directional RNA Library Prep Kit for Illumina (E7420; New England Biolabs, Ipswich, MA, USA). During library preparation, cDNAs were enriched by 12-cycle PCR. Illumina HiSeq 2500 was used to perform 50 bp single-end sequencing according to the manufacturer's instructions. RNA-Seq data were deposited in the DNA Data Bank of Japan (DDBJ) Sequence Read Archive (DRA). Sequencing reads obtained from directional RNA-Seq were assessed using the FASTX tool kit (Patel et al., 2012) to remove short (< 20 bp) and low quality (quality score < 20) reads, followed by trimming of the adaptor sequence. Preprocessed reads were mapped to the mouse mm10 genome using TopHat2/Bowtie2 (Kim et al., 2013). After converting the bam file to a bed file, the intersect function in bedtools2 (Quinlan and Hall, 2010) was used for removal of PCR duplicates and calculating reads per kb of exon model per million model-transcript-mapped reads (RPKM). Differentially expressed genes (DEGs) were ranked based on the rowVars function in the genefilter R package (genefilter: methods for filtering genes from high-throughput experiments; R package version 1.56.0.). Expression level differences were determined using R with the pheatmap package (pheatmap: Pretty Heatmaps; R package version 1.0.10.).

2.10. Embryoid body formation

Chimpanzee iPSCs were dissociated with TrypLE Express and 1×10^6 cells/ml were transferred to 6-well low attachment culture plates (3471; Corning Inc., Corning, New York, NY, USA) in 15% FBS/DMEM. After 2 weeks culture, iPSC-derived embryoid bodies (EB) were transferred to Geltrex-coated plates and cultured in adhesion conditions with 15% FBS/DMEM for another 2 weeks.

2.11. Direct neurosphere formation and neuronal differentiation culture

Direct neurosphere formation culture was performed according to a previous report (Nakai et al., 2018). Briefly, chimpanzee iPSCs were dissociated with TrypLE Express and 1.5×10^5 cells/ml were transferred to 6-well low attachment culture plates in KBM Neural Stem Cell medium (16050200; Kohjin Bio, Saitama, Japan) supplemented with 10 μM Y-27632. The next day, 2 μM dorsomorphin (11967; Cayman Chemical Company, Ann Arbor, MI, USA), 10 μM SB431542 (13031; Cayman Chemical Company), 1 ng/ml Stembeads FGF2 (SB500; StemCultures, Rensselaer, NY, USA), and 1 × B-27 supplement (17504044; Gibco) were added to the medium. Half the medium was changed on day 4. To induce neuronal differentiation, neurospheres were plated onto Geltrex-coated culture plates and cultured for 2 weeks in KBM Neural Stem Cell medium without FGF2 and epidermal growth factor (EGF) but supplemented with 1 × B-27 supplement.

3. Results

3.1. Generation of chimpanzee iPSCs with plasmid vectors under feeder-free culture

To generate chimpanzee iPSCs, we performed gene transduction and culture of skin fibroblasts according to the experimental procedure in Fig. 1A and referring to published protocols of human iPSCs (Okita et al., 2011; Chen et al., 2011; Mali et al., 2010). Chimpanzee skin fibroblasts were derived from one male (0363M) and two female (0274F and 0138F) adult individuals. Plasmids bearing six reprogramming factors (human OCT3/4, SOX2, KLF4, L-MYC, LIN28, and shRNA against *TP53*) were transduced into primary fibroblasts by lipofection (Okita et al., 2011). EGFP expression showed successful gene transduction with high efficiency (Fig. 1B). Six days after lipofection, the medium was replaced with medium containing hydrocortisone to improve proliferation of fibroblasts (Chen et al., 2011). Ten days after lipofection, the medium was replaced again with medium containing sodium butyrate to enhance cellular reprogramming (Mali et al., 2010). iPSC colonies appeared 20–30 days after lipofection (Fig. 1C). These iPSC colonies were picked and expanded on laminin-511E8 fragment-coated dishes using a defined medium (Nakagawa et al., 2014). Under feeder cell-free conditions, we established five iPSC lines from three individuals: 0363M-1, 0363M-2, 0274F-1, 0274F-2, and 0138F-1. Similar to human iPSCs, chimpanzee iPSCs formed flat and round colonies, and exhibited a high nuclear-to-cytoplasmic ratio (Fig. 1D). The iPSCs maintained a normal karyotype over 20 passages (Fig. 1E). Growth of chimpanzee iPSCs was dependent on FGF2. Accordingly, iPSCs grew robustly in the presence of FGF2 while maintaining a typical colony morphology and alkaline phosphatase activity. Contrarily, their growth was abrogated and alkaline phosphatase activity lost in the absence of FGF2 (Fig. 1F). Genomic PCR detected genomic integration of the *OCT3/4* transgene in three iPSC lines (0363M-1, 0274F-1, and 0138F-1), but there was no obvious genomic integration of any other transgene in all iPSC lines (Fig. 1G).

3.2. Expression of pluripotency-associated genes in chimpanzee iPSCs

During expansion culture under feeder-free conditions, iPSC colonies maintained strong and homogeneous alkaline phosphatase activity (Fig. 2A). Immunofluorescence analysis of chimpanzee iPSCs (0138F-1) revealed expression of pluripotency-associated intracellular antigens including OCT3/4, NANOG, SOX2, SALL4, LIN28, and DPPA4 proteins (Fig. 2B). Pluripotency-associated cell surface antigens (namely, TRA-1-81, SSEA3, SSEA4, and E-cadherin) were also expressed in chimpanzee iPSCs (Fig. 2C), as described for human iPSCs (Takahashi et al., 2007). Beside these markers, a R-10G sugar chain epitope is highly enriched in human embryonic stem cells (ESCs) and iPSCs, but not embryonal carcinoma cells. This epitope can therefore be used as a molecular indicator of highly reprogrammed iPSCs (Kawabe et al., 2013). Chimpanzee iPSCs were homogeneously positive for the R-10G epitope, indicating a fully pluripotent state. Another pluripotency-associated sugar chain epitope has been detected using rBC2LCN lectin staining (Tateno et al., 2013; Onuma et al., 2013). Similar expression of pluripotency antigens was also observed in the other chimpanzee iPSC lines (0363M-2 and 0274F-2) (Supplementary Figures S1 and S2).

The expression profile of pluripotency-associated genes was further

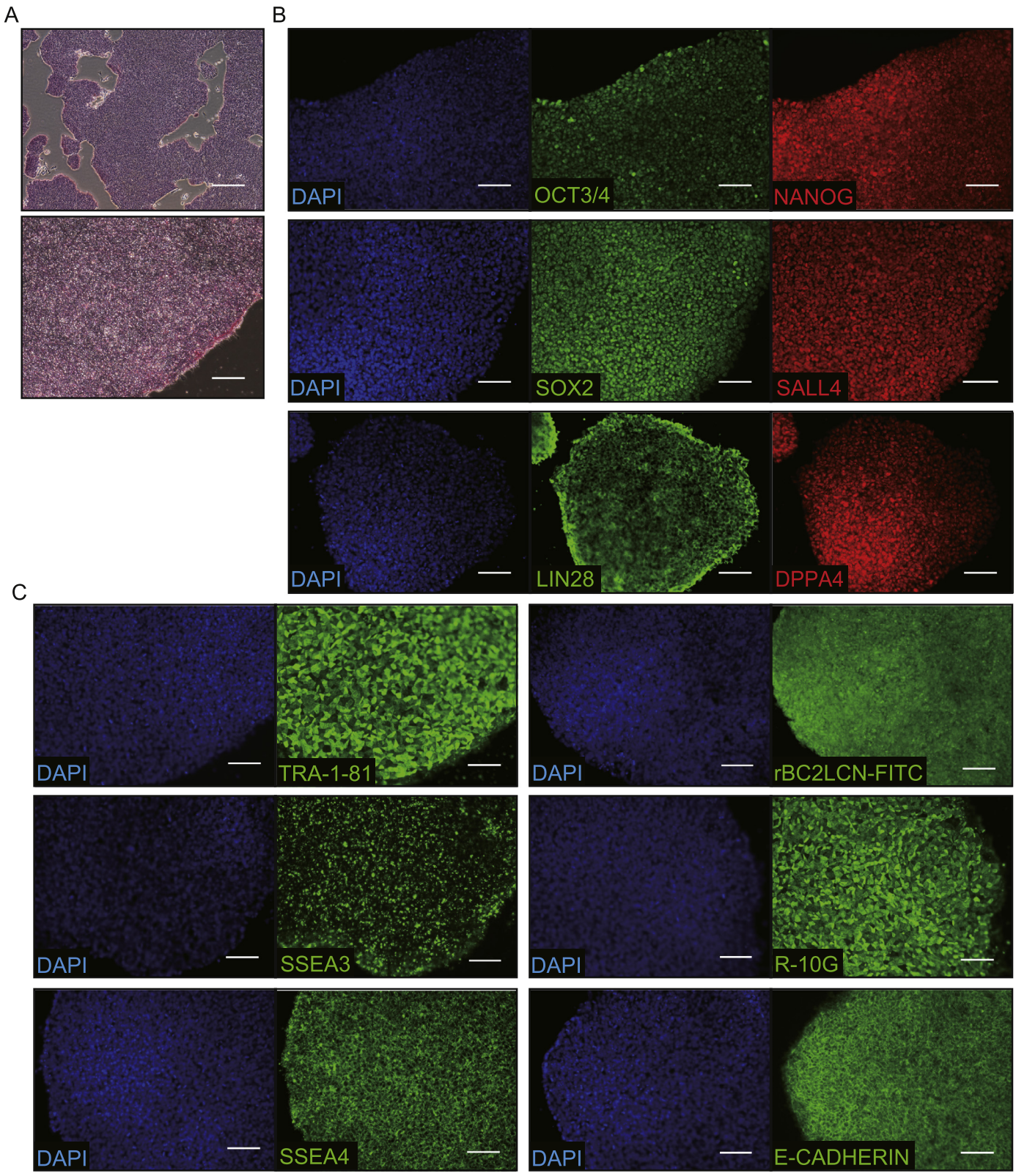

Fig. 2. Immunofluorescence analysis of pluripotency antigens in chimpanzee iPSCs.
A. Alkaline phosphatase activity of chimpanzee iPSCs (0138F-1). Scale bars: 500 μm (upper) and 100 μm (lower). B. Expression of pluripotency-related intracellular antigens. Scale bar: 100 μm. C. Expression of pluripotency-related cell membrane antigens. Scale bar: 100 μm. Nuclei were counterstained with DAPI.

characterized by RT-PCR analysis. Regarding iPSC reprogramming factors, endogenous expression of *OCT3/4, SOX2, LIN28*, and *L-MYC* was induced in iPSCs, whereas *KLF4* was downregulated compared with parental fibroblasts upon reprogramming. Many pluripotency marker genes (including *NANOG, GDF3*, and *REX1*) were upregulated in all iPSC lines (Fig. 3). Upregulated genes also included *DNMT3B, GRB7, NODAL*, and *PODXL*, which are pluripotency genes expressed in human ESCs and iPSCs in a primed pluripotent state (Takahashi et al., 2007)

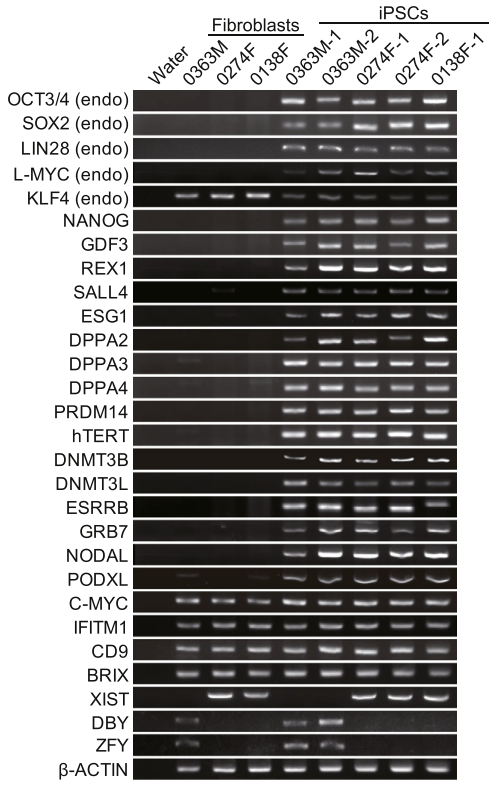

Fig. 3. Expression of pluripotency genes in chimpanzee iPSCs.
RT-PCR analyses of pluripotency-associated genes in five chimpanzee iPSC lines (0363M-1, 0363M-2, 0274F-1, 0274F-2, and 0138F-1) and three parental fibroblast lines (0363M, 0274F, and 0138F). β-actin was used as an internal control. Water was used as a negative control.

(Fig. 3). Expression of *XIST, DBY*, and *ZFY* determined the sexual origin of each cell type: female chimpanzee-derived fibroblasts and iPSCs expressed *XIST*, while male chimpanzee-derived cells expressed *DBY* and *ZFY*.

3.3. Embryoid body-mediated differentiation of chimpanzee iPSCs

Next, we examined differentiation ability of chimpanzee iPSCs into three germ layers by EB formation culture. Three iPSC lines from different individuals (0363M-2, 0274F-2, and 0138F-1) were selected and cultured in suspension conditions in FBS-containing differentiation medium (Fig. 4A–C, Supplementary Figures S3A–C and S4A–C). After 2-weeks of culture, ball-shaped EBs were transferred to gelatin-coated culture plates. Various types of spontaneously differentiated cells grew around the attached EBs. Immunofluorescence analysis identified cells positive for the ectoderm (nestin, βIII tubulin), mesoderm (α-SMA, vimentin), and endoderm (SOX17, AFP) markers in EB outgrowths (Fig. 4D). Compared with 0138F-1 iPSCs, 0363M-2 and 0274F-2 iPSCs exhibited less neural differentiation, as demonstrated by nestin and βIII tubulin immunofluorescence (Supplementary Figures S3D and S4D).

It was previously reported that human iPSCs have a different differentiation propensity in a donor-dependent manner (Kajiwara et al., 2012; Nishizawa et al., 2016; Cahan and Daley, 2013). Therefore, we performed RT-PCR analysis to further characterize differentiated EB outgrowths among chimpanzee iPSC lines. These EB outgrowths expressed marker genes of the ectoderm (e.g., *NEUROD1, DCX*), mesoderm (e.g., *NKX2.5, MSX1*), and endoderm (e.g., *AFP, CDX2*), while expression of pluripotency genes (i.e., *OCT3/4, NANOG, REX1*) was totally abolished (Fig. 4E, Supplementary Figures S3E and S4E). Moreover, the gene expression profile was different among iPSC lines. In particular, consistent with the immunofluorescence data, expression of neural genes such as *PAX6* was prominent in EB outgrowths derived from 0138F-1 but not from 0363M-2 and 0274F-2 iPSCs. Thus, we primarily chose 0138F-1 iPSCs for the following experiments of directed differentiation into neural lineages.

3.4. Direct neurosphere formation culture of chimpanzee iPSCs

To reconstruct early neural development from chimpanzee iPSCs, we used direct neurosphere formation culture (Nakai et al., 2018) in combination with dorsomorphin and SB431542, both of which are chemical inhibitors against BMP and transforming growth factor-β signaling, and which promote neural differentiation from pluripotent stem cells (Morizane et al., 2011; Chambers et al., 2009). 0138F-1 iPSCs were dissociated into single cells and directly transferred into suspension cultures (Fig. 5A). The iPSC-derived neurospheres grew progressively during 1-week of culture with FGF2, EGF, dorsomorphin, and SB431542 stimulation. Addition of leukemia inhibitory factor (LIF) was likely to have a supportive effect on sphere formation. Neurosphere formation was abrogated in the presence of chemical inhibitors against phosphoinositide 3-kinase (PI3K) or signal transducers and activators of transcription (STAT) (Supplementary Figure S5). Neuronal differentiation was induced when neurospheres had outgrown in adherent conditions without FGF2 and EGF for 2 weeks. Immunofluorescence analysis of the neurosphere outgrowths detected bipolar-shaped cells positive for neuroepithelial cell and/or radial glia markers (i.e., SOX2, PAX6, OTX2, FOXG1, nestin, vimentin, and BRN2) and neurons (βIII tubulin, MAP2, and drebrin) (Fig. 5B, C, Supplementary Figure S6) but not astrocytes (S100β) (data not shown). Astrocyte differentiation was induced when neurospheres had outgrown in the presence of EGF for 4 weeks (Supplementary Figure S7). Similar neural differentiation was observed by direct neurosphere formation culture of 0363M-2 and 0274F-2 iPSCs, albeit slightly less differentiation by EB formation culture (Supplementary Figures S8 and S9).

3.5. Gene expression and developmental dynamics during neurosphere formation culture

To characterize changes in gene expression during the course of direct neurosphere formation, we performed RNA-Seq analysis of transcriptomes of chimpanzee iPSCs and spheres on day 1, 3, 5, and 7 cultures (Fig. 6A). DEGs particularly enriched neural development-associated genes (Supplementary Figures S10, S11, S12). Hierarchical clustering of DEGs classified the cells into three distinct groups (Fig. 6B). Group 1 encompasses iPSCs and day 1 spheres. This group was the first to separate from the others, which were then separated into groups 2 (day 3 spheres) and 3 (day 5 and 7 spheres). Principal component analysis revealed that day 3 spheres were at an intermediate stage between groups 1 and 3 (Fig. 6C). Quantitative RT-PCR analysis of selected DEGs and key developmental regulators showed sequential gene expression changes during neurosphere formation (Fig. 6D). Upon neurosphere formation culture, expression of the pluripotent epiblast markers, *NANOG* and *NODAL*, was still present but halved on day 1 and nearly abolished until day 3. Subsequently, cadherin switching from E-cadherin to N-cadherin proceeded on day 3. Expression of early neural development regulators also began to be upregulated from day 3. *ZFHX1B* and *MEIS2* were intensely induced on day 3 and further augmented on day 7. *ZNF521* was moderately upregulated on day 3 but strongly on day 5. Marked upregulation on day 5 was also observed for *OTX1, EMX2, PAX6*, and *FOXG1*. Eventually, on day 7, sharp upregulation of *NR2F1* and *NR2F2* was detected. Similar upregulation was also observed on day 7 for *HES5* and other Notch and Wnt signal transducers (Supplementary Figure S10). In addition to these known developmental regulators, which are essential for early neural development, we also identified DEGs with stage-specific transient upregulation. Accordingly, *IGFBP6, ABHD12B*, and *CHGA* were highly expressed on day 1, while *CUZD1* showed transient expression specifically on day 3 (Fig. 6E,

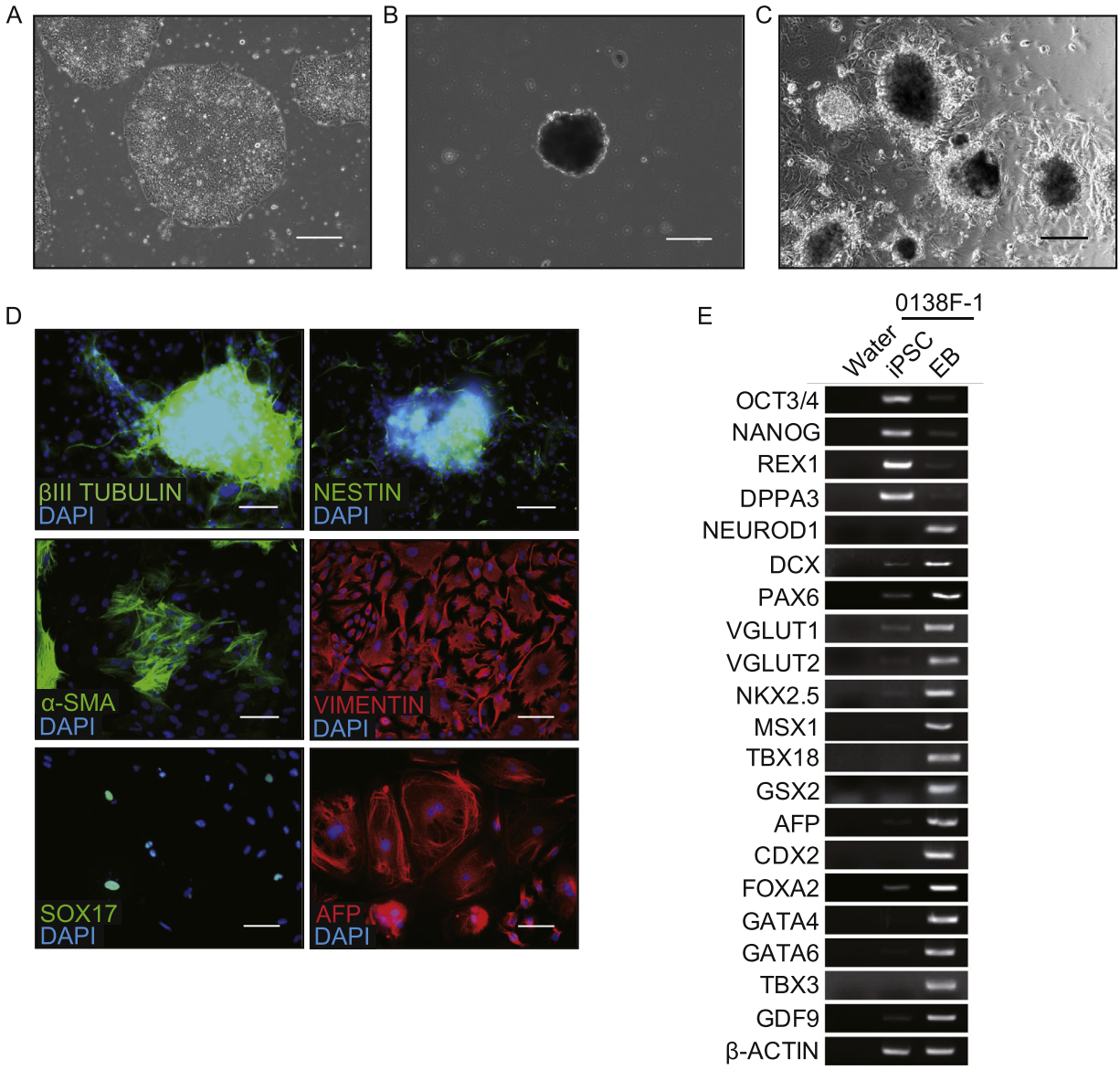

Fig. 4. Embryoid body formation culture of chimpanzee iPSCs.
A. Chimpanzee iPSCs (0138F-1) before embryoid body (EB) formation culture. B. iPSC-derived EBs after 2-weeks of suspension culture. C. Outgrowth of EBs after 2-weeks of adherent culture. Scale bar: 200 μm. D. Immunofluorescence analyses of markers for the ectoderm (βIII tubulin, nestin), mesoderm (α-SMA, vimentin), and endoderm (SOX17, AFP). Nuclei were counterstained with DAPI. Scale bar: 100 μm. E. RT-PCR analyses of pluripotency and differentiation marker genes for EB outgrowth. β-actin was used as an internal control. Water was used as a negative control.

Supplementary Figure S10).

Consistent with the gene expression kinetics, the neurospheres underwent developmental fate transition along with the culture period. Spheres from day 1, 3, 5, and 7 cultures were transferred to adherent neuronal differentiation conditions, and immunofluorescence analyses performed after 14 days of subsequent culture (Fig. 7A). Nestin$^+$ cells were observed in every condition, but their morphology was different according to the sphere culture period (Fig. 7B). Day 1 spheres produced enlarged mesenchymal nestin$^+$ cells, whereas day 3 sphere-derived nestin$^+$ cells were composed of a smaller radial cell population. Most nestin$^+$ cells emerged from day 5 and 7 spheres, and further exhibited bipolar morphology with extension of radial fibers. BRN2$^+$ cells appeared in only a fraction of the nestin$^+$ cell population from day 3 spheres but were dominant from day 5 and 7 spheres. Furthermore, βIII tubulin$^+$MAP2$^+$ neuronal differentiation was inactive until day 3, but then active in 5 day sphere cultures (Supplementary Figure S13). To determine whether the developmental potential of spheres proceeded during neurosphere formation or was simply attributed to the total culture period, we next adjusted the total culture period by extending the neuronal differentiation culture according to each sphere culture (Fig. 7C). Again, the developmental potential changed progressively depending on neurosphere formation but not total cell culture period (Fig. 7D, Supplementary Figure S13). Thus, early neural development proceeds during neurosphere formation culture of chimpanzee iPSCs, in which neurogenic potential is acquired between day 3 and 5 spheres.

4. Discussion

Evolution of human neural development is a classical and major concern in biology. To address this, it is essential to determine the molecular and cellular foundations of neural development in humans and our close relative, the chimpanzee, for comparative analyses. Here, iPSC technology allows an *in vitro* model system to access and manipulate neural development, while avoiding technical and ethical

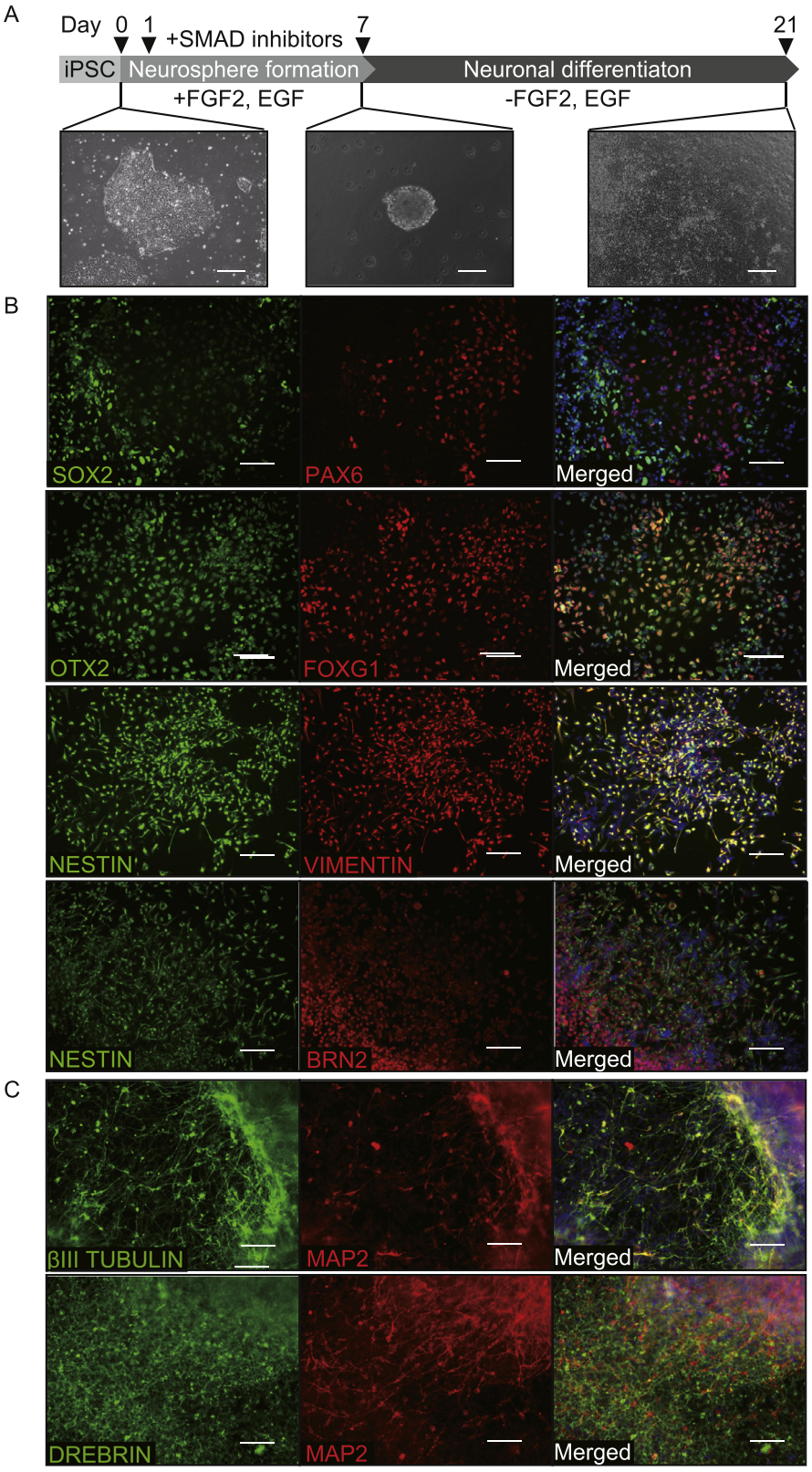

Fig. 5. Direct neurosphere formation culture of chimpanzee iPSCs.
A. Schematic design of neural differentiation culture of chimpanzee iPSCs. Phase contrast images show chimpanzee iPSCs (0138F-1) before neurosphere formation culture (Scale bar: 200 μm), iPSC-derived neurospheres after 7-days of suspension culture (Scale bar: 100 μm), and neuronal differentiation of neurospheres after 2-weeks of adherent culture (Scale bar: 200 μm). B. Immunofluorescence analyses of neural stem cell markers. Scale bar: 100 μm. C. Immunofluorescence analyses of neuronal markers. Scale bar: 100 μm. Nuclei were counterstained with DAPI.

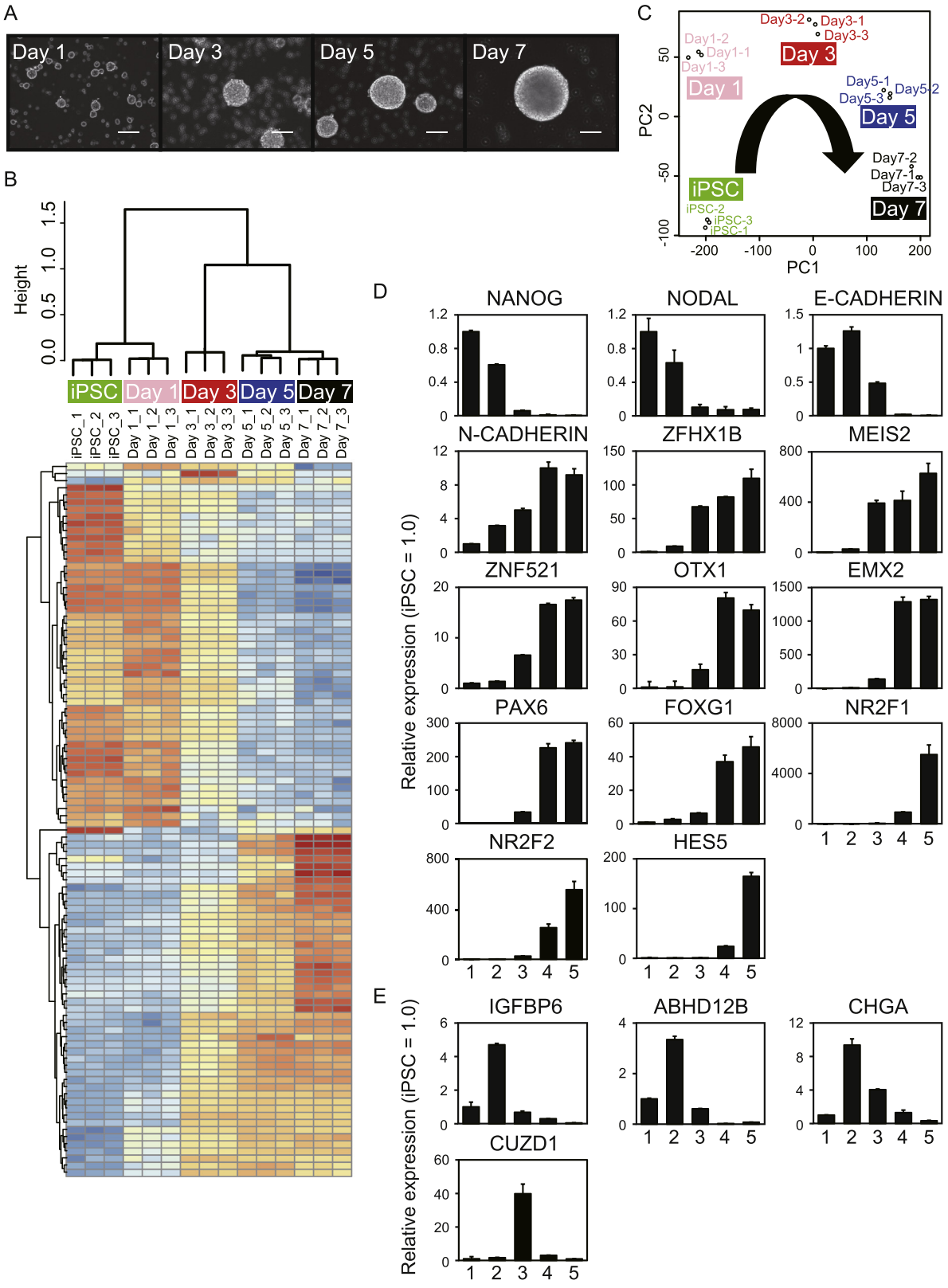

Fig. 6. Sequential gene expression shifts during neurosphere formation.
A. Phase contrast images of sequential neurosphere formation from chimpanzee iPSCs. Scale bar: 100 μm. B. Hierarchical clustering of iPSC and neurosphere replicates using expression matrix of differentially expressed genes (DEGs) identified by RNA-Seq analyses. DEGs were ranked based on the rowVars function in the genefilter R package. Note that 100 top-ranked highly variable genes among samples clearly discriminated the developmental stages (iPSCs and day 1, 3, 5, 7 of neurosphere formation cultures). C. Principal component analysis of DEGs. D. Real-time PCR analyses of key developmental regulator genes during early neural development. E. Real-time PCR analyses of DEGs newly identified by RNA-Seq. Expression of each gene was normalized to β-actin. Results represent relative expression levels normalized to iPSCs.

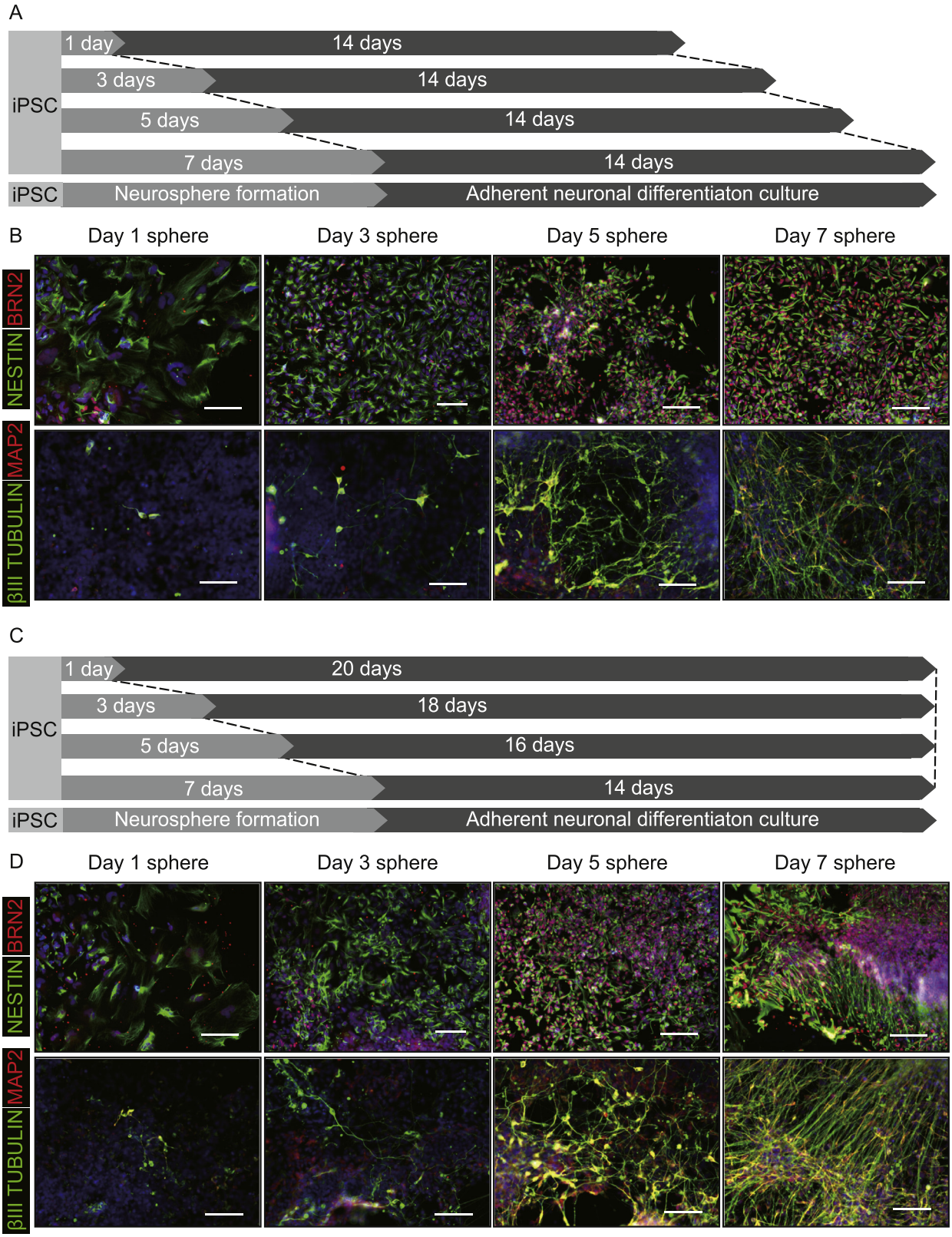

Fig. 7. Time course of developmental potency of neurospheres.
A. Schematic design of time course of direct neurosphere formation and subsequent duration-fixed (14 days) neuronal differentiation cultures of chimpanzee iPSCs. B. Immunofluorescence analyses of neural stem cell (nestin, BRN2) and neuronal (βIII tubulin, MAP2) markers after duration-fixed neuronal differentiation culture of each sphere. Scale bar: 100 μm. C. Schematic design of time course of direct neurosphere formation and subsequent duration-flexible (14–20 days) neuronal differentiation cultures of chimpanzee iPSCs. D. Immunofluorescence analyses of neural stem cell (nestin, BRN2) and neuronal (βIII tubulin, MAP2) markers after duration-flexible neuronal differentiation culture of each sphere. Scale bar: 100 μm. Nuclei were counterstained with DAPI.

restrictions that are associated with *in vivo* studies of humans and chimpanzees (Suzuki and Vanderhaeghen, 2015). Consequently, there has been an increasing interest in recent years of research into Evo-Devo studies of human traits using iPSCs. To date, several chimpanzee iPSCs have been generated (Marchetto et al., 2013; Fujie et al., 2014; Gallego Romero et al., 2015). Nonetheless, compared with previous studies, the chimpanzee iPSC cultures that we have established here have technical advantages such as easier methods (including lipofection-based plasmid transduction), comprehensive feeder-free culture for generating and maintaining iPSCs, and simple and rapid directed neural differentiation. Because Evo-Devo study of human traits has primarily attracted the interest of researchers such as evolutionary biologists, who are not familiar with stem cell cultures, technical convenience is a critical element to launch an iPSC-based Evo-Devo study. Our conventional chimpanzee iPSC cultures will enable many researchers to undertake human Evo-Devo studies using *in vitro* stem cells.

The pluripotency of iPSCs can be classified into two major states known as naïve and primed pluripotency that reflect differences in developmental stages (Nichols and Smith, 2009). Unlike mouse iPSCs with naïve pluripotency, default pluripotency of human and non-human primate iPSCs is fixed in a primed state. Likewise, chimpanzee iPSCs exhibited the characteristic features of primed pluripotency in colony morphology (Fig. 1D), growth factor requirement (Fig. 1F), pluripotency antigen expression (Fig. 2C), and X chromosome inactivation (Fig. 3), similar to human iPSCs. In addition, the differentiation capacity assessed by EB formation varied among chimpanzee iPSC lines (Fig. 4, Supplementary Figures S3 and S4). Variations in differentiation capacity have been extensively validated among human iPSC lines, and this variability is ascribed to several factors including genetic differences of donors, epigenetic memory of parental cells, and aberrations during reprogramming process (Cahan and Daley, 2013). It would be also the case in chimpanzee iPSCs, therefore functional validation of iPSC lines is necessary for understanding clonal differences.

To recapitulate early neural development from chimpanzee iPSCs, we used direct neurosphere formation culture with chemical inhibitors. This straightforward method yielded rapid and efficient induction of NSCs (Fig. 5), as with Japanese macaque iPSCs (Nakai et al., 2018). Time course analyses of neurosphere formation revealed that chimpanzee iPSC-derived spheres underwent sequential early neural development during 1-week of culture (Figs. 6 and 7). Given hallmark gene expression and neuronal differentiation potency, stepwise developmental progression in neurosphere formation is likely to encompass determination of two major cell fates. The first fate determination happened between day 1 and 3 spheres (Fig. 6B). During this period, expression of pluripotent epiblast genes diminished whereas early neural development genes began to be expressed (Fig. 6D, Supplementary Figure S10). The early expressed genes included an epiblast-to-neuroectoderm determinant, *ZFHX1B* (Chng et al., 2010), and a neuroectoderm-competence gene, *ZNF521* (Kamiya et al., 2011). Additionally, cadherin switching from E-cadherin to N-cadherin, which is a diagnostic event in neuroectoderm specification (Stemmler, 2008), was also detected at this timing. Regarding the cellular phenotype, day 3 spheres efficiently generated neuroepithelial nestin$^+$ cells instead of enlarged mesenchymal nestin$^+$ cells differentiated from day 1 spheres (Fig. 7). These results suggest that the first cell fate determination reflects neuroepithelial commitment from a late epiblast state. Subsequently, the second fate determination happened between day 3 and 5 spheres (Fig. 6B). At this timing, expression of radial glia-related genes (such as *PAX6*, which drives radial glia formation from neuroepithelial cells (Suter et al., 2009)) was activated (Fig. 6D, Supplementary Figure S10). Following upregulation of Notch and Wnt signal transducers indicates activation of these essential signaling pathways for specification and expansion of neurogenic radial glia (Kageyama et al., 2008; Harrison-Uy and Pleasure, 2012). These gene expression shifts were associated with differentiation potential of sphere-derived cells. Compared with day 3 sphere-derived cells, bipolar shapes with radial processes became evident in nestin$^+$BRN2$^+$ cells derived from day 5 and 7 spheres (Fig. 7). Neuronal differentiation also became active between day 3 and 5 spheres (Supplementary Figure S13). Thus, the second fate determination may result in differentiation of neuroepithelial cells into radial glia with acquisition of a neurogenic potential. Taken together, it is conceivable that direct neurosphere formation culture of chimpanzee iPSCs recapitulates ontogenetic cell fate determination in early neural development from the late epiblast (day 1) to neuroepithelial cells (day 3) and neurogenic radial glia (days 5–7).

The developmental model in chimpanzee neurosphere formation is partly compatible with previous mouse studies, which specified a stepwise early NSC development from ESCs or embryos by neurosphere formation culture (Tropepe et al., 2001; Hitoshi et al., 2004; Akamatsu et al., 2009). In these mouse models, the earliest spheres, called primitive NSCs (pNSCs), are representative of late epiblast cells, which still express OCT3/4 and have the ability to differentiate to non-neural lineages. pNSCs then lose their pluripotency and transition into neural lineage-committed definitive NSCs (dNSCs), indicative of neural tube and embryonic brain stages. Accordingly, the first fate determination between day 1 and 3 chimpanzee spheres may correspond with the pNSC-dNSC transition in mice. The self-renewal of mouse dNSCs is initially FGF2-dependent but turns to be EGF-dependent. Since our direct neurosphere formation culture contained both FGF2 and EGF consistently, it remains unclear whether chimpanzee iPSC-derived neurospheres undergo such a transition in growth factor requirement. However, given that Notch signaling promotes the transition from FGF-dependent to EGF-dependent dNSCs (Akamatsu et al., 2009), it may happen on day 7 or later during direct neurosphere formation culture of chimpanzee iPSCs (Fig. 6D, Supplementary Figure S10).

Based on stepwise differentiation by direct neurosphere formation culture, RNA-Seq analysis enabled us to monitor temporal shifts of gene expression profiles during the course of iPSC differentiation to neurogenic radial glia. We were also able to identify novel DEGs that may function in early neural development. High expression of *IGFBP6, ABHD12B*, and *CHGA* was detected in day 1 spheres, while *CUZD1* was specifically expressed in day 3 spheres (Fig. 6E). These genes might contribute to developmental regulation of cell fate decision in early neural development. For example, *CUZD1* acts as a signal mediator of the Janus kinase (JAK)/STAT pathway, and enhances cell proliferation in mammary epithelium development (Mapes et al., 2017). Increased expression of *CUZD1* causes breast cancer tumorigenesis due to overgrowth of mammary epithelial cells (Mapes et al., 2018). Alternatively, it is known that the JAK/STAT pathway promotes pNSC proliferation in response to LIF (Hitoshi et al., 2004) and also maintenance of neurogenic NSCs in response to FGF2 (Yoshimatsu et al., 2006). Indeed, STAT inhibitors abrogated neurosphere formation from chimpanzee iPSCs (Supplementary Figure S5) as demonstrated in human ESCs-derived neurospheres (Sherry-Lynes et al., 2017). Therefore, *CUZD1* may regulate neuroepithelial cell proliferation via the JAK/STAT pathway in a developmental stage-specific manner. Since direct neurosphere formation culture is applicable to Japanese macaques (Nakai et al., 2018) and humans (data not shown), comparative analyses among primate species will uncover the molecular foundation unique to human early neural development. [2]iPSC-based *in vitro* differentiation systems also enable functional analyses of genes that may be responsible for human traits. Accumulating knowledge of comparative genomic and transcriptomic studies have revealed part of the human-specific molecular footprint as human-specific genes or enhancers (Heide et al., 2017; Levchenko et al., 2018) that may yield differential gene functions and/or expression patterns unique to human brain development. Several studies have challenged us to substantiate possible links between human-specific genomic changes and evolutionary traits. Indeed, human-specific expression of *TBC1D3* (Ju et al., 2016), *ARHGAP11B*

[2] Please begin on a New line here.

(Florio et al., 2015; Florio et al., 2016), *NOTCH2NL* (Suzuki et al., 2018; Florio et al., 2018), and *FDZ8* (Boyd et al., 2015) were shown to augment proliferation ability of NSCs and progenitor cells, potentially contributing to expansion of the human cerebral cortex. These developmental functions were assessed by ectopic expression in the mouse embryonic brain. However, there are still large biological differences between focally humanized mice and humans, therefore it is difficult to discuss the physiological function of human-specific genes by referring to ectopic expression in mice (Mitchell and Silver, 2018). Considering phylogenic and genomic similarity, chimpanzee iPSC-based *in vitro* differentiation provides a more biologically related model system to evaluate the causal relationship between human genotypes and developmental phenotypes (Prescott et al., 2015; Otani et al., 2016; Mora-Bermudez et al., 2016; Field et al., 2019; Marchetto et al., 2019; Pollen et al., 2019). A recent study examined the developmental effect of human-specific *NOTCH2NL* using *in vitro* differentiation culture of mouse and human ESCs (Fiddes et al., 2018). This showed that ectopic expression of *NOTCH2NL* resulted in delayed neuronal differentiation in mice whereas its deletion by genome editing caused accelerated differentiation of neural progenitors in human. These challenges with human and chimpanzee iPSCs will shed light on functional and phenotypic effects of human-specific genes one-by-one and hold the promise to uncover human brain evolution.

CRediT authorship contribution statement

Ryunosuke Kitajima: Methodology, Investigation, Funding acquisition. **Risako Nakai:** Methodology, Validation, Investigation, Formal analysis, Data curation, Funding acquisition. **Takuya Imamura:** Methodology, Software, Validation, Investigation, Formal analysis, Data curation, Funding acquisition. **Tomonori Kameda:** Software, Investigation, Formal analysis. **Daiki Kozuka:** Investigation. **Hirohisa Hirai:** Validation, Investigation, Resources, Funding acquisition. **Haruka Ito:** Investigation. **Hiroo Imai:** Validation, Resources, Funding acquisition. **Masanori Imamura:** Conceptualization, Methodology, Validation, Investigation, Data curation, Writing - original draft, Writing - review & editing, Visualization, Supervision, Project administration, Funding acquisition.

Declaration of Competing Interest

The authors have no conflicts of interest to declare.

Acknowledgments

We thank the staff at Kumamoto Sanctuary, Tama Zoological Park, Beppu Cable Rakutenchi, Primate Research Institute, and the Great Ape Information Network (GAIN) for chimpanzee materials. We also thank Zachary Yu-Ching Lin, Yohei Bamba, Yohei Okada, Hideyuki Okano, Kota Kuroki, Sawako Okada, Takumi Kato, Yuriko Hirai, and Kaori Yasutake for technical assistance and other support. We thank Rachel James, Ph.D., from Edanz Group (www.edanzediting.com/ac) for editing a draft of this manuscript. This work was supported by grants from the Japan Society for the Promotion of Science (JSPS); Leave a Nest Grants (Life Technologies Japan Award, On-chip Biotechnologies Award, SCREEN Holdings Award, L-RAD Award); Interuniversity Bio-Backup Project for Basic Biology; Brain Sciences Project of the Center for Novel Science Initiatives (CNTI), National Institutes of Natural Sciences (NINS); Aichi Cancer Research Foundation; Takeda Science Foundation; Kyoto University Foundation; Hori Science and Arts Foundation; Cooperation Research Program of the Primate Research Institute, Kyoto University; Extramural Collaborative Research Grant of Cancer Research Institute, Kanazawa University; and the Cooperative Study Program of National Institute for Physiological Sciences. R.N. was supported by the DAIKO Foundation and the Kyoto University Graduate School of Science Fund.

Supplementary materials

Supplementary material associated with this article can be found, in the online version, at doi:10.1016/j.scr.2020.101749.

References

Akamatsu, W., DeVeale, B., Okano, H., Cooney, A.J., van der Kooy, D., 2009. Suppression of Oct4 by germ cell nuclear factor restricts pluripotency and promotes neural stem cell development in the early neural lineage. J. Neurosci. 29, 2113–2124.
Borrell, V., Reillo, I., 2012. Emerging roles of neural stem cells in cerebral cortex development and evolution. Dev. Neurobiol. 72, 955–971.
Boyd, J.L., Skove, S.L., Rouanet, J.P., Pilaz, L.J., Bepler, T., Gordan, R., Wray, G.A., Silver, D.L., 2015. Human-chimpanzee differences in a FZD8 enhancer alter cell-cycle dynamics in the developing neocortex. Curr. Biol. 25, 772–779.
Cahan, P., Daley, G.Q., 2013. Origins and implications of pluripotent stem cell variability and heterogeneity. Nat. Rev. Mol. Cell Biol. 14, 357–368.
Chambers, S.M., Fasano, C.A., Papapetrou, E.P., Tomishima, M., Sadelain, M., Studer, L., 2009. Highly efficient neural conversion of human ES and iPS cells by dual inhibition of SMAD signaling. Nat. Biotechnol. 27, 275–280.
Chen, G., Gulbranson, D.R., Hou, Z., Bolin, J.M., Ruotti, V., Probasco, M.D., Smuga-Otto, K., Howden, S.E., Diol, N.R., Propson, N.E., Wagner, R., Lee, G.O., Antosiewicz-Bourget, J., Teng, J.M., Thomson, J.A., 2011. Chemically defined conditions for human iPSC derivation and culture. Nat. Methods 8, 424–429.
Cheng, Z., Ventura, M., She, X., Khaitovich, P., Graves, T., Osoegawa, K., Church, D., DeJong, P., Wilson, R.K., Paabo, S., Rocchi, M., Eichler, E.E., 2005. A genome-wide comparison of recent chimpanzee and human segmental duplications. Nature 437, 88–93.
Chng, Z., Teo, A., Pedersen, R.A., Vallier, L., 2010. SIP1 mediates cell-fate decisions between neuroectoderm and mesendoderm in human pluripotent stem cells. Cell Stem Cell 6, 59–70.
Fiddes, I.T., Lodewijk, G.A., Mooring, M., Bosworth, C.M., Ewing, A.D., Mantalas, G.L., Novak, A.M., van den Bout, A., Bishara, A., Rosenkrantz, J.L., Lorig-Roach, R., Field, A.R., Haeussler, M., Russo, L., Bhaduri, A., Nowakowski, T.J., Pollen, A.A., Dougherty, M.L., Nuttle, X., Addor, M.C., Zwolinski, S., Katzman, S., Kriegstein, A., Eichler, E.E., Salama, S.R., Jacobs, F.M.J., Haussler, D., 2018. Human-specific NOTCH2NL genes affect notch signaling and cortical neurogenesis. Cell 173, 1356–1369 e1322.
Field, A.R., Jacobs, F.M.J., Fiddes, I.T., Phillips, A.P.R., Reyes-Ortiz, A.M., LaMontagne, E., Whitehead, L., Meng, V., Rosenkrantz, J.L., Olsen, M., Hauessler, M., Katzman, S., Salama, S.R., Haussler, D., 2019. Structurally conserved primate lncrnas are transiently expressed during human cortical differentiation and influence cell-type-specific genes. Stem Cell Reports 12, 245–257.
Florio, M., Albert, M., Taverna, E., Namba, T., Brandl, H., Lewitus, E., Haffner, C., Sykes, A., Wong, F.K., Peters, J., Guhr, E., Klemroth, S., Prufer, K., Kelso, J., Naumann, R., Nusslein, I., Dahl, A., Lachmann, R., Paabo, S., Huttner, W.B., 2015. Human-specific gene ARHGAP11B promotes basal progenitor amplification and neocortex expansion. Science 347, 1465–1470.
Florio, M., Heide, M., Pinson, A., Brandl, H., Albert, M., Winkler, S., Wimberger, P., Huttner, W.B., Hiller, M., 2018. Evolution and cell-type specificity of human-specific genes preferentially expressed in progenitors of fetal neocortex. Elife 7.
Florio, M., Namba, T., Paabo, S., Hiller, M., Huttner, W.B., 2016. A single splice site mutation in human-specific ARHGAP11B causes basal progenitor amplification. Sci. Adv. 2, e1601941.
Fujie, Y., Fusaki, N., Katayama, T., Hamasaki, M., Soejima, Y., Soga, M., Ban, H., Hasegawa, M., Yamashita, S., Kimura, S., Suzuki, S., Matsuzawa, T., Akari, H., Era, T., 2014. New type of Sendai virus vector provides transgene-free iPS cells derived from chimpanzee blood. PLoS ONE 9, e113052.
Gallego Romero, I., Pavlovic, B.J., Hernando-Herraez, I., Zhou, X., Ward, M.C., Banovich, N.E., Kagan, C.L., Burnett, J.E., Huang, C.H., Mitrano, A., Chavarria, C.I., Friedrich Ben-Nun, I., Li, Y., Sabatini, K., Leonardo, T.R., Parast, M., Marques-Bonet, T., Laurent, L.C., Loring, J.F., Gilad, Y., 2015. A panel of induced pluripotent stem cells from chimpanzees: a resource for comparative functional genomics. Elife 4, e07103.
Harrison-Uy, S.J., Pleasure, S.J., 2012. Wnt signaling and forebrain development. Cold Spring Harb. Perspect. Biol. 4, a008094.
Heide, M., Long, K.R., Huttner, W.B., 2017. Novel gene function and regulation in neocortex expansion. Curr. Opin. Cell Biol. 49, 22–30.
Hitoshi, S., Seaberg, R.M., Koscik, C., Alexson, T., Kusunoki, S., Kanazawa, I., Tsuji, S., van der Kooy, D., 2004. Primitive neural stem cells from the mammalian epiblast differentiate to definitive neural stem cells under the control of Notch signaling. Genes Dev. 18, 1806–1811.
Ju, X.C., Hou, Q.Q., Sheng, A.L., Wu, K.Y., Zhou, Y., Jin, Y., Wen, T., Yang, Z., Wang, X., Luo, Z.G., 2016. The hominoid-specific gene TBC1D3 promotes generation of basal neural progenitors and induces cortical folding in mice. Elife 5.
Kageyama, R., Ohtsuka, T., Kobayashi, T., 2008. Roles of Hes genes in neural development. Dev. Growth Differ. 50 (suppl 1), S97–103.
Kajiwara, M., Aoi, T., Okita, K., Takahashi, R., Inoue, H., Takayama, N., Endo, H., Eto, K., Toguchida, J., Uemoto, S., Yamanaka, S., 2012. Donor-dependent variations in hepatic differentiation from human-induced pluripotent stem cells. Proc. Natl. Acad. Sci. U. S. A. 109, 12538–12543.
Kamiya, D., Banno, S., Sasai, N., Ohgushi, M., Inomata, H., Watanabe, K., Kawada, M., Yakura, R., Kiyonari, H., Nakao, K., Jakt, L.M., Nishikawa, S., Sasai, Y., 2011. Intrinsic transition of embryonic stem-cell differentiation into neural progenitors. Nature 470, 503–509.

Kawabe, K., Tateyama, D., Toyoda, H., Kawasaki, N., Hashii, N., Nakao, H., Matsumoto, S., Nonaka, M., Matsumura, H., Hirose, Y., Morita, A., Katayama, M., Sakuma, M., Furue, M.K., Kawasaki, T., 2013. A novel antibody for human induced pluripotent stem cells and embryonic stem cells recognizes a type of keratan sulfate lacking oversulfated structures. Glycobiology 23, 322–336.

Kim, D., Pertea, G., Trapnell, C., Pimentel, H., Kelley, R., Salzberg, S.L., 2013. TopHat2: accurate alignment of transcriptomes in the presence of insertions, deletions and gene fusions. Genome Biol. 14, R36.

Kriegstein, A., Noctor, S., Martinez-Cerdeno, V., 2006. Patterns of neural stem and progenitor cell division may underlie evolutionary cortical expansion. Nat. Rev. Neurosci. 7, 883–890.

Kronenberg, Z.N., Fiddes, I.T., Gordon, D., Murali, S., Cantsilieris, S., Meyerson, O.S., Underwood, J.G., Nelson, B.J., Chaisson, M.J.P., Dougherty, M.L., Munson, K.M., Hastie, A.R., Diekhans, M., Hormozdiari, F., Lorusso, N., Hoekzema, K., Qiu, R., Clark, K., Raja, A., Welch, A.E., Sorensen, M., Baker, C., Fulton, R.S., Armstrong, J., Graves-Lindsay, T.A., Denli, A.M., Hoppe, E.R., Hsieh, P., Hill, C.M., Pang, A.W.C., Lee, J., Lam, E.T., Dutcher, S.K., Gage, F.H., Warren, W.C., Shendure, J., Haussler, D., Schneider, V.A., Cao, H., Ventura, M., Wilson, R.K., Paten, B., Pollen, A., Eichler, E.E., 2018. High-resolution comparative analysis of great ape genomes. Science 360.

Levchenko, A., Kanapin, A., Samsonova, A., Gainetdinov, R.R., 2018. Human accelerated regions and other human-specific sequence variations in the context of evolution and their relevance for brain development. Genome. Biol. Evol. 10, 166–188.

Mali, P., Chou, B.K., Yen, J., Ye, Z., Zou, J., Dowey, S., Brodsky, R.A., Ohm, J.E., Yu, W., Baylin, S.B., Yusa, K., Bradley, A., Meyers, D.J., Mukherjee, C., Cole, P.A., Cheng, L., 2010. Butyrate greatly enhances derivation of human induced pluripotent stem cells by promoting epigenetic remodeling and the expression of pluripotency-associated genes. Stem Cells 28, 713–720.

Mapes, J., Anandan, L., Li, Q., Neff, A., Clevenger, C.V., Bagchi, I.C., Bagchi, M.K., 2018. Aberrantly high expression of the CUB and zona pellucida-like domain-containing protein 1 (CUZD1) in mammary epithelium leads to breast tumorigenesis. J. Biol. Chem. 293, 2850–2864.

Mapes, J., Li, Q., Kannan, A., Anandan, L., Laws, M., Lydon, J.P., Bagchi, I.C., Bagchi, M.K., 2017. CUZD1 is a critical mediator of the JAK/STAT5 signaling pathway that controls mammary gland development during pregnancy. PLos Genet. 13, e1006654.

Marchetto, M.C., Hrvoj-Mihic, B., Kerman, B.E., Yu, D.X., Vadodaria, K.C., Linker, S.B., Narvaiza, I., Santos, R., Denli, A.M., Mendes, A.P., Oefner, R., Cook, J., McHenry, L., Grasmick, J.M., Heard, K., Fredlender, C., Randolph-Moore, L., Kshirsagar, R., Xenitopoulos, R., Chou, G., Hah, N., Muotri, A.R., Padmanabhan, K., Semendeferi, K., Gage, F.H., 2019. Species-specific maturation profiles of human, chimpanzee and bonobo neural cells. Elife 8.

Marchetto, M.C.N., Narvaiza, I., Denli, A.M., Benner, C., Lazzarini, T.A., Nathanson, J.L., Paquola, A.C.M., Desai, K.N., Herai, R.H., Weitzman, M.D., Yeo, G.W., Muotri, A.R., Gage, F.H., 2013. Differential L1 regulation in pluripotent stem cells of humans and apes. Nature 503, 525–529.

Merkle, F.T., Alvarez-Buylla, A., 2006. Neural stem cells in mammalian development. Curr. Opin. Cell Biol. 18, 704–709.

Mitchell, C., Silver, D.L., 2018. Enhancing our brains: genomic mechanisms underlying cortical evolution. Semin. Cell Dev. Biol. 76, 23–32.

Mora-Bermudez, F., Badsha, F., Kanton, S., Camp, J.G., Vernot, B., Kohler, K., Voigt, B., Okita, K., Maricic, T., He, Z., Lachmann, R., Paabo, S., Treutlein, B., Huttner, W.B., 2016. Differences and similarities between human and chimpanzee neural progenitors during cerebral cortex development. Elife 5.

Morizane, A., Doi, D., Kikuchi, T., Nishimura, K., Takahashi, J., 2011. Small-molecule inhibitors of bone morphogenic protein and activin/nodal signals promote highly efficient neural induction from human pluripotent stem cells. J. Neurosci. Res. 89, 117–126.

Nakagawa, M., Taniguchi, Y., Senda, S., Takizawa, N., Ichisaka, T., Asano, K., Morizane, A., Doi, D., Takahashi, J., Nishizawa, M., Yoshida, Y., Toyoda, T., Osafune, K., Sekiguchi, K., Yamanaka, S., 2014. A novel efficient feeder-free culture system for the derivation of human induced pluripotent stem cells. Sci. Rep. 4, 3594.

Nakai, R., Ohnuki, M., Kuroki, K., Ito, H., Hirai, H., Kitajima, R., Fujimoto, T., Nakagawa, M., Enard, W., Imamura, M., 2018. Derivation of induced pluripotent stem cells in Japanese macaque (Macaca fuscata). Sci. Rep. 8, 12187.

Nichols, J., Smith, A., 2009. Naive and primed pluripotent states. Cell Stem Cell 4, 487–492.

Nishizawa, M., Chonabayashi, K., Nomura, M., Tanaka, A., Nakamura, M., Inagaki, A., Nishikawa, M., Takei, I., Oishi, A., Tanabe, K., Ohnuki, M., Yokota, H., Koyanagi-Aoi, M., Okita, K., Watanabe, A., Takaori-Kondo, A., Yamanaka, S., Yoshida, Y., 2016. Epigenetic variation between human induced pluripotent stem cell lines is an indicator of differentiation capacity. Cell Stem Cell 19, 341–354.

Okita, K., Matsumura, Y., Sato, Y., Okada, A., Morizane, A., Okamoto, S., Hong, H., Nakagawa, M., Tanabe, K., Tezuka, K., Shibata, T., Kunisada, T., Takahashi, M., Takahashi, J., Saji, H., Yamanaka, S., 2011. A more efficient method to generate integration-free human iPS cells. Nat. Methods 8, 409–412.

Onuma, Y., Tateno, H., Hirabayashi, J., Ito, Y., Asashima, M., 2013. rBC2LCN, a new probe for live cell imaging of human pluripotent stem cells. Biochem. Biophys. Res. Commun. 431, 524–529.

Otani, T., Marchetto, M.C., Gage, F.H., Simons, B.D., Livesey, F.J., 2016. 2D and 3D stem cell models of primate cortical development identify species-specific differences in progenitor behavior contributing to brain size. Cell Stem Cell 18, 467–480.

Ozair, M.Z., Kintner, C., Brivanlou, A.H., 2013. Neural induction and early patterning in vertebrates. Wiley Interdiscip. Rev. Dev. Biol. 2, 479–498.

Patel, R.K., Jain, M., 2012. NGS QC Toolkit: a toolkit for quality control of next generation sequencing data. PLoS ONE 7, e30619.

Pollen, A.A., Bhaduri, A., Andrews, M.G., Nowakowski, T.J., Meyerson, O.S., Mostajo-Radji, M.A., Di Lullo, E., Alvarado, B., Bedolli, M., Dougherty, M.L., Fiddes, I.T., Kronenberg, Z.N., Shuga, J., Leyrat, A.A., West, J.A., Bershteyn, M., Lowe, C.B., Pavlovic, B.J., Salama, S.R., Haussler, D., Eichler, E.E., Kriegstein, A.R., 2019. Establishing cerebral organoids as models of human-specific brain evolution. Cell 176, 743–756 e717.

Prescott, S.L., Srinivasan, R., Marchetto, M.C., Grishina, I., Narvaiza, I., Selleri, L., Gage, F.H., Swigut, T., Wysocka, J., 2015. Enhancer divergence and cis-regulatory evolution in the human and chimp neural crest. Cell 163, 68–83.

Quinlan, A.R., Hall, I.M., 2010. BEDTools: a flexible suite of utilities for comparing genomic features. Bioinformatics 26, 841–842.

Sherry-Lynes, M.M., Sengupta, S., Kulkarni, S., Cochran, B.H., 2017. Regulation of the JMJD3 (KDM6B) histone demethylase in glioblastoma stem cells by STAT3. PLoS ONE 12, e0174775.

Stemmler, M.P., 2008. Cadherins in development and cancer. Mol. Biosyst. 4, 835–850.

Suter, D.M., Tirefort, D., Julien, S., Krause, K.H., 2009. A Sox1 to Pax6 switch drives neuroectoderm to radial glia progression during differentiation of mouse embryonic stem cells. Stem Cells 27, 49–58.

Suzuki, I.K., Gacquer, D., Van Heurck, R., Kumar, D., Wojno, M., Bilheu, A., Herpoel, A., Lambert, N., Cheron, J., Polleux, F., Detours, V., Vanderhaeghen, P., 2018. Human-specific NOTCH2NL genes expand cortical neurogenesis through Delta/Notch regulation. Cell 173, 1370–1384 e1316.

Suzuki, I.K., Vanderhaeghen, P., 2015. Is this a brain which I see before me? Modeling human neural development with pluripotent stem cells. Development 142, 3138–3150.

Takahashi, K., Tanabe, K., Ohnuki, M., Narita, M., Ichisaka, T., Tomoda, K., Yamanaka, S., 2007. Induction of pluripotent stem cells from adult human fibroblasts by defined factors. Cell 131, 861–872.

Tateno, H., Matsushima, A., Hiemori, K., Onuma, Y., Ito, Y., Hasehira, K., Nishimura, K., Ohtaka, M., Takayasu, S., Nakanishi, M., Ikehara, Y., Ohnuma, K., Chan, T., Toyoda, M., Akutsu, H., Umezawa, A., Asashima, M., Hirabayashi, J., 2013. Podocalyxin is a glycoprotein ligand of the human pluripotent stem cell-specific probe rBC2LCN. Stem Cells Transl. Med. 2, 265–273.

Tropepe, V., Hitoshi, S., Sirard, C., Mak, T.W., Rossant, J., van der Kooy, D., 2001. Direct neural fate specification from embryonic stem cells: a primitive mammalian neural stem cell stage acquired through a default mechanism. Neuron 30, 65–78.

Yoshimatsu, T., Kawaguchi, D., Oishi, K., Takeda, K., Akira, S., Masuyama, N., Gotoh, Y., 2006. Non-cell-autonomous action of STAT3 in maintenance of neural precursor cells in the mouse neocortex. Development 133, 2553–2563.

Yunis, J.J., Sawyer, J.R., Dunham, K., 1980. The striking resemblance of high-resolution G-banded chromosomes of man and chimpanzee. Science 208, 1145–1148.